Journal of Engineering and Applied Sciences 13 (Special Issue 8): 6431-6439, 2018
ISSN: 1816-949X

Mathematical and Numerical Modeling of Free Turning Segments of Self-Regulated Static-Dynamic Gas Bearing

[1]Vladimir N. Beschastnyh, [2]Mikhail P. Bulat, [2]Alexander A. Gorbachev and [2]Igor A. Volobuev
[1]Scientific and Production Association "Lianozovo Electromechanical Plant",
127411 Moscow, Russia
[2]University ITMO, 197101 Saint Petersburg, Russia

Abstract: We have studied a self-regulating radial gas-dynamic bearing and developed a methodology for its calculation and design. We have also developed modeling methods for rotational segments of the bearing surface stable in terms of rotation angle, load and rotor speed. There was developed a numerical method for determining the position of a segment with zero moments as well as the method of analyzing its stability in this position. This study describes a technique to determine the stable equilibrium position of a segment. We have determined the values and directions of a torque and the resultant forces for different values of the average thickness of the lubricating layer and the shaft speed. There were obtained the pressure plots in the lubricating layer of the segment. We have defined the parametric dependences of design characteristics of the bearing on the load and on the rotational speed of the shaft. Practical srelevance. The developed calculation technique can be used in designing hybrid air bearings while selecting the position of a segment rotation axis. Segment rotation allows the range of self-regulation of air bearings to be extended and in certain limits to parry the overloads on the shaft.

Key words: Numerical simulation, self-regulating radial static-dynamic, gas bearing, segment's steady position, torque, net force

INTRODUCTION

The purpose of this study is to develop a methodology for designing rotational segments of the bearing surface of hybrid gas bearings that are stable in terms of rotation angle, load and rotor velocity.

In recent years, interest in gas bearings has increased significantly. The theory of classical gas bearings is well developed. The fundamental works by Sheinberg and Shisheyev (1979) and Constantinescu (1963) as well as the works of Kotlyar (1967), Zablotsky *et al.* (1970), Loitsiansky and Stepanyants (1967) are dedicated to this problem.

Based on the method of creating bearing capacity, there are Gas-Static (GSB), Gas-Dynamical (GDB) and hybrid Gas-Static-Dynamic Bearings (GSDB) (Bulat and Bulat, 2013). In GDB, lifting force is created by the interaction between the moving parts of a shaft and a bearing with a viscous thin layer of gas lubricant. Their main drawback is small load capacity, limited by the lifting force which is created by the Bernoulli and Poiseuille effects. At a shaft rotation frequency lesser than the designed one, GDB operate in dry friction mode which causes its early run-out.

GSB require a constant supply of working gas into the gap between the bearing's housing and the rotor in order to create a lifting force. In addition, GSB is characterized by various oscillatory regimes caused by the mismatch between the gas flow entering the lubricating gap and the one flowing out of it through the ends of the bearing.

The scientific novelty is that each segment of the bearing support surface must be self-aligning in other words the segment which is under the influence of a pressure drop and the turning torque, must be installed at a certain angle in relation to the shaft surface. The main difference between the methods described in the work from existing solutions is to find such an arrangement of each segment's rotation axis which will ensure its stability in terms of the rotation angle. Typically, segments of the hybrid gas bearing are controlled by a control system or a variety of damping systems (Nelson and Hollingsworth, 1977). In this case, it is necessary to calculate the forces and moments at the freely rotating segments of hybrid air bearing. Below is a description of a design procedure for the rotary segments of the bearing's surface which are stable in terms of rotation angle, load and rotor velocity, as well as the numerical method for determining the

Corresponding Author: Vladimir N. Beschastnyh, Scientific and Production Association "Lianozovo Electromechanical Plant", 127411 Moscow, Russia

segment's position at which the moments applied to it equal zero. Demonstrational calculations were performed. The results are compared with estimates made by asymptotic methods as well as with the experiment results.

MATERIALS AND METHODS

Mathematical model of a lubricating layer

The initial system of equations for a radial bearing: Usually, there is used a basic equation of hydrodynamic theory of lubrication the Reynolds equation when analyzing the flow in the lubricating layer (Reynolds, 1886). Reynolds equation is derived from the assumption that the lubricating layer is thin. Let us consider a full-radius radial bearing of finite length l and elongation $\lambda = l/d$ where d is the diameter. The Reynolds equation for it in the polar coordinate system is written as:

$$\frac{\partial}{\partial\phi}(\bar{h}^3\frac{\partial\bar{p}}{\partial\phi})+\frac{1}{4\lambda^2}\frac{\partial}{\partial\bar{z}}(\bar{h}^3\frac{\partial\bar{p}}{\partial\bar{z}}) = 6\frac{\partial\bar{h}}{\partial\phi}+12\frac{\partial\bar{h}}{\partial t} \quad (1)$$

where, $\bar{h} = h/c$, $\bar{p} = p/p$ and the meaning of the remaining notations. Let us introduce the dimensionless variables:

$$\bar{z} = \frac{z}{\ell},\ \bar{p} = \frac{p}{p_*},\ p_* = \frac{\mu\omega r^2}{c^2},\ \bar{t} = \omega t \quad (2)$$

Where:

ω = The rotor's angular velocity
$\mu = \nu\rho$ = The dynamic viscosity
ν = The kinematic viscosity
ρ = Density

We can write an equation for a relative gap:

$$\bar{h} = 1-\varepsilon\cos(\varphi-\theta),\ \varepsilon = \frac{e}{c} \quad (3)$$

By differentiating Eq. 3 with respect to t and φ, we obtain:

$$\frac{\partial\bar{h}}{\partial t} = -\frac{\partial\varepsilon}{\partial t}\cos(\varphi-\theta)-\varepsilon\frac{\partial\theta}{\partial t}\sin(\varphi-\theta)$$
$$\partial\bar{h}/\partial\varphi = \varepsilon\sin(\varphi-\theta) \quad (4)$$

Based on the Omitted values of second order of smallness (ε^2) and Eq. 4, Eq. 1 in dimensionless variables (Eq. 2) can be rewritten as:

$$\frac{\partial^2\bar{p}}{\partial\varphi^2}+\frac{1}{4\lambda^2}\frac{\partial^2\bar{p}}{\partial\bar{z}^2} = 6(1-2\frac{\partial\theta}{\partial t})\varepsilon\sin(\varphi-\theta)-12\frac{\partial\varepsilon}{\partial t}\cos(\varphi-\theta) \quad (5)$$

Equation 5 can be integrated for specified values of pressure at the bearing's ends p1 and p2:

$$\bar{p} = [-6(1-2\frac{\partial\theta}{\partial t})\varepsilon\sin(\varphi-\theta)+ 12\frac{\partial\varepsilon}{\partial t}\cos(\varphi-\theta)]\Phi(\bar{z})+\bar{p}_1-(\bar{p}_1-\bar{p}_2)\bar{z}, \quad (6)$$

Based on Eq. 6, we can then obtain the expression for the resultant forces in the projection on axes e and θ:

$$\bar{P}_e = P_e/P_a = -6\pi k_p\frac{\partial\varepsilon}{\partial t} \quad (7)$$

$$\bar{P}_\theta = P_\theta/P_a = 3\pi k_p(1-2\frac{\partial\theta}{\partial t})\varepsilon \quad (8)$$

where, $k_p = 1-th\lambda/\lambda$ is a coefficient which is equal to one for an infinitely long bearing (without any leaks) and $k_p \approx \lambda^2/3$ for a very short bearing with $\lambda << 1$. Eq. 6-8 provide an exact solution for the non-stationary lubrication layer of a full-radius radial bearing and are suitable for developing a technique used for calculating the shaft's non-stationary motion.

$$\frac{\partial}{\partial x}\left(ph^3\frac{\partial p}{\partial x}\right)+\frac{\partial}{\partial z}\left(ph^3\frac{\partial p}{\partial z}\right) = 12\mu\frac{\partial}{\partial t}(ph)+6\mu\frac{\partial}{\partial x}(puh) \quad (9)$$

Where:

p = The pressure
h = The gap
u = Velocity
t = Time
μ = Viscosity
x = The coordinate oriented along the generating line of the shaft
z = The coordinate oriented along the shaft's axis

Reason for verifying the Reynolds Model: The practice of calculating gas-static bearings has shown that the throttles, through which the gas lubricant is fed into the gap as well as micro-grooves designed to distribute gas along the supporting surface must sometimes be included into calculation area. The flow at the boundary of the throttles and micro-grooves is essentially three-dimensional. In addition, at near-critical regimes when the velocity of gas flowing out from the throttle is close to the sonic speed, inertia forces cannot be neglected. Thus, results obtained by solving Eq. 9 must be verified with a numerical model based on the solution of Navier-Stokes equations (Beschastnykh,

2011). The flow within a thin layer can be considered as laminar (Beschastnykh and Ilyina, 2015). Therefore, equations are not averaged and turbulence models are not used.

Asymptotic approximations

Approximation of a two-dimensional lubricating layer: A number of important estimates can be obtained on the assumption that the shaft is infinitely long and the size of the bearing in shaft's direction is infinite as well. Then, the flow in the lubricating layer can be considered as two-dimensional and flat. Thus, derivatives can be neglected with respect to z. In the stationary case, we can neglect the derivatives with respect to t, then Eq. 9 can be written as:

$$\frac{\partial}{\partial x}\left(ph^3\frac{\partial p}{\partial x}\right)=6\mu\frac{\partial}{\partial x}(puh) \tag{10}$$

Let us consider a bearing with the length d in the direction of x-axis, located in the environment with the gas pressure p_a. Then, the following parameters can be introduced, the gap size h_{in}, through which the lubricant flows into the bearing and the gap size h_{out}, through which the lubricant flows out. Thus, the bearing will be characterized by certain average gap size h_0. If the gap is much smaller than the length d then the following reasoning is also applicable to a bearing with the curved generating line. For example, it can be a segmented radial bearing. Then, d is the arc length of the segment's inner surface generating line, h_{in} is the gap between segment's frontal edge and the shaft and h_{out} is the gap between segment's rear edge and the shaft. If the bearing is a full-radius one with an eccentricity of e, then d is the length of the trunnion circle, $h_{in}= h_0+e/2$, $h_{out} = h_0-e/2$. Thus, the following conclusions are valid for all types of bearings. In dimensionless variables, Eq. 10 can be written as:

$$\frac{\partial}{\partial \bar{x}}\left(\bar{p}\bar{h}^3\frac{\partial \bar{p}}{\partial \bar{x}}\right)=\Lambda\frac{\partial}{\partial \bar{x}}(\bar{p}\bar{h})\Lambda=\frac{6\mu vd}{H^2p_a} \tag{11}$$

where, Λ is the Harrison parameter or the dimensionless bearing characteristic. Let us introduce the parameter $A = h_{in}/h_0$ the relative thickness of the entrance gap. Then, if we consider (Eq. 11 and 10) will be finally written as:

$$\frac{\partial p}{\partial x}=\Lambda\frac{1}{\left(A+2x(1-A)\right)^2}\left(1-\frac{C}{p\left(A+2x(1-A)\right)}\right) \tag{12}$$

Dashes denoting the dimensionlessness of the variable will not further be written for simplicity. Equation 12 is a nonlinear partial differential equation that must be solved numerically which was apparently, first done by Sternlicht (1961) and Raimondi (1961). At present, the Reynolds equations are solved by standard numerical methods in most commercial gas-dynamic packages, for example, in ANSYS CFX. The practice of applying Eq. 12 shows that it adequately describes the pressure change far from the segment's edges and with high accuracy on the segment's symmetry plane perpendicular to the shaft's axis.

Applying asymptotic methods allows obtaining sufficiently meaningful conclusions about the behavior of gas bearings with real rather than idealized design schemes.

Kotlyar has developed the asymptotic methods in the most general form: first for a cylindrical lubricating layer, then for a spherical one and subsequently they were generalized for a surface of arbitrary shape. We will consider the limiting cases $\Lambda\to 0$ and $\Lambda\to\infty$.

Approximation of simulation operation in gas-static regime ($\Lambda\to 0$). If $\Lambda\to 0$, then the relative pressure will be $p\to 1$. This allows us to eliminate p from Eq. 12 and integrate this Eq. 13:

$$p=\Lambda\left(\frac{\left(x^2-x\right)(1-A)}{\left(A+2x(1-A)\right)^2}\right)+1 \tag{13}$$

Based on Eq. 13, we can determine the load capacity of a bearing section with the length d and width L, namely the load capacity of a separate bearing segment:

$$W = Ldp_aK_\Gamma,\quad K_\Gamma=\frac{\Lambda}{4(A-1)}\left(\frac{1}{(A-1)}1\right.\\ \left.n\left(\frac{A}{(2-A)}\right)-2\right) \tag{14}$$

where, K_G is the specific load capacity of the bearing. K_G is strongly increasing with $A\to 2$ in other words when the output gap tends to zero. With increasing Λ, specific load capacity also increases. A similar Eq. 14 can be obtained for a full-radius bearing:

$$W=2rLp_a\frac{\Lambda\pi\varepsilon}{\left(2+\varepsilon^2\right)\sqrt{1-\varepsilon^2}} \tag{15}$$

Where:

$\varepsilon = e/c$ = The relative eccentricity

c = The mean size of the radial gap

Based on the graphs and Eq. 13 and 14, it is not difficult to conclude that GSB segments capable of

turning to a certain angle with respect to the bearing surface have angular rigidity in the angle of rotation. Indeed, a change in the angle leads to the pressure diagram distortion. At that, pressure decreases in places where the gap grows and increases where the gap becomes smaller. It should be noted that the presence of angular rigidity does not yet guarantee the segment stability in terms of rotation angle. Approximation of simulation operation in gas-dynamic regime ($\Lambda \to \infty$). If there is no loss of generality, we can assume that in this case u¬8. Thus, we are dealing with either GDB or with GSDB in a regime where the influence of the blowing is not determinative. This allows us to integrate Eq. 12:

$$p = \frac{A}{A+2x(1-A)} \quad (16)$$

Equation 16 shows that pressure in the gap varies monotonically as well as the max pressure in the output section and the ratio between the maximum and minimum pressure is equal to the ratio between the input and output gaps. Based on the above, load capacity of the gas-dynamic bearing will be different from zero only when the surfaces are positioned at an angle:

$$W = Ldp_a K_\Gamma, \quad K_\Gamma = \frac{1}{2(A-1)} \ln\left(\frac{A}{(2-A)}\right) - 1 \quad (17)$$

In the case of a full-radius radial bearing when the shaft and the trunnion are positioned with eccentricity. Thus, Eq. 17 can be written as:

$$W = 2rLp_a \pi \sqrt{1+\frac{2}{3}\varepsilon^2}\left(\sqrt{\frac{1}{1-\varepsilon^2}} - 1\right)\frac{1}{\varepsilon} \quad (18)$$

In addition, it is impossible to draw an a priori conclusion about the segment's stability in terms of rotation angle. In this case, we need to find a point on the segment's surface at which the total moment of pressure forces (Eq. 18) will be zero:

$$x_h = \frac{1}{\ln\frac{(2-A)}{A}} - \frac{A}{2(1-A)} \quad (19)$$

Hence, the greater is the desired load capacity in gas dynamic regime (the larger is the ratio between the input and the output gaps), the closer must be the segment rotation axis to the output section (Eq. 19) in order for it to be stationary. In this case, the segment will be stable in terms of rotation angle because the angle's decrease shifts the pressure diagram to the right from the hinge axis and the segment tends to increase the angle. As the angle decreases, the situation is the opposite.

Thus, considering the two limiting cases $\Lambda \to \infty$ and $\Lambda \to 0$ simulating gas-dynamic and gas-static regimes, respectively, we can draw conclusions about the behavior of a real segmented GSDB in which the final reaction is the sum of gas-static and gas-dynamic components.

RESULTS AND DISCUSSION

Practical implementation with numerical simulation methods

The numerical method: Numerical modeling was carried out with Ansys CFX package within the Reynolds model framework, verification calculations were performed with the OpenFoam package by solving the Navier-Stokes equations for laminar, compressible, heat-conducting and viscous gas.

Calculation area and boundary conditions: The idea of GSDB geometry and the calculation area are illustrated in Fig. 1. The air is supplied into the inlet at a pressure of 6 bar and a temperature of 300 K. The pressure is set equal to 1 bar along the segment perimeter (boundary conditions). The shaft rotates at a specified frequency relative to the axis: 5000, 10.000, 20.000, 30.000 and 42.000 rpm. There are specified solid wall boundary conditions for non-flow, adherence and thermal insulation.

Calculation area is divided into three bodies in order to build a grid, lubricating gap, a microgroove and a supply tube with a throttle. A microgroove and a throttle form a nozzle.

Algorithm for calculating the stable position of a segment: We have considered that the pressure is constant at the inlet and the average gap, determined by the shaft's load, changes. The segment's slope angle is set by the minimum output gap which size varies within the specified limits. The pressure distribution, the segment's load capacity and the gas flow through the throttles are the results of calculation. In addition, the moment of pressure force acting on the segment in relation to the rotation axis is determined based on calculation results. At the same time, we understand that in reality, the segment of GSDB is aligned by itself at the certain angle. In this case, the moment must be equal to zero. The calculation sequence is as follows:

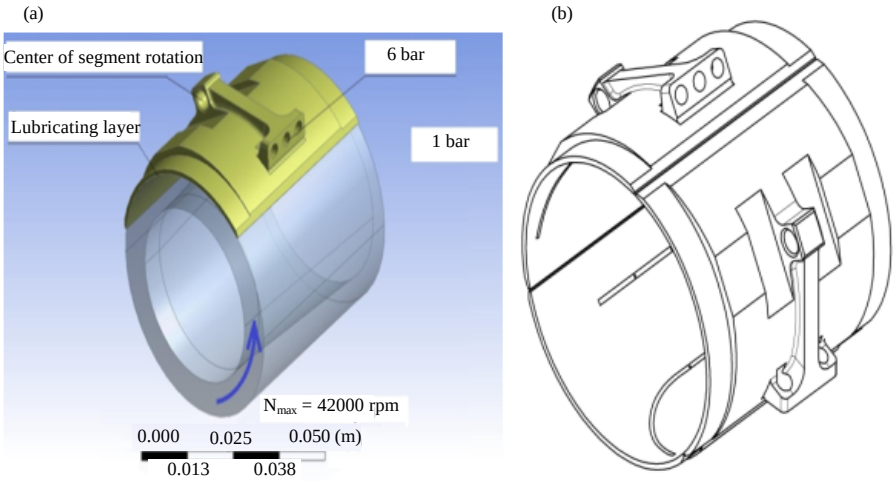

Fig. 1: a) Radial bearing and b) Geometric model of the working area for calculating the lubricating layer between the bearing's segment and the shaft

- Setting the average gap between the shaft and the segment H_0 at such point, above which the axis of rotation is located (Fig. 1b). In our case, the values of H_0 are of 10, 15, 20 and 25 μm
- Creating 3-D Models with different gap tapering (with a different value of the output gap h_{out}) for the selected parameters. There must be at least three different values
- Based on 3-D Models, generating difference grid and performing numerical calculation of the flow in the lubricating gap at different shaft rotation velocities. As the result, we get the diagrams of pressure distribution at the segment
- Based on the pressure diagrams, determining the torque at the segment's rotation axis and the resultant of pressure forces at the segment
- Plotting dependences of forces and moments on the output gap h_{out}
- Based on these diagrams, determining (by linear interpolation) the output gap at which segment's position is equilibrium (M = 0) and the resultant of pressure forces (F_0) is at the segment in equilibrium position
- Analyzing the derivative of the moment with respect to the rotation angle in the equilibrium position. If the derivative is negative then the equilibrium position is stable

Asymptotic analysis of boundary load capacity: F_i is the resultant of pressure forces applied to segment's rotation axis. In a full-radius bearing, pressure in the lubricating layer changes continuously and has a resultant force F directed opposite to the shaft axis e displacement and determining the load capacity of the entire bearing. In a segment bearing, situation is more complicated. Each segment has its own resultant F_i. The total load capacity is determined by the vector addition of these forces. The condition for providing the load capacity of the rotor's support can be written as follows:

$$F = kMg + F_D + F_p < W \quad (20)$$

Where:
F_D = The dynamic component of the force
F_p = The gas-static component

$h_{out} > h_{min}$ where, h_{min} is the minimum gap between the shaft and the bearing, M is the rotor's mass, W Bearing's load capacity, k the coefficient taking into account the effect of mass forces.

Based on the formulas of the gas lubrication theory for a gas bearing, we transform the expression (Eq. 20) into the:

$$2\frac{\pi r}{2} L p_a \left(\frac{A}{2(A-1)} \ln \frac{A}{2-A} - 1 \right) \left(1 - \frac{1}{z^2} \right) \quad (21)$$
$$\frac{180^\circ}{z} = kMg + F_D + F_p$$

Where:
L = The bearing's length
P_a = Bearing pressure
z = The number of segments in the bearing

Based on Eq. 21, we express the value of bearing pressure for a full-radius bearing:

$$p_a = \frac{F}{dLK_\Gamma} = \frac{kMg+F_D+F_p}{dL\pi\sqrt{1+\frac{2}{3}\varepsilon^2}\left[\sqrt{\frac{1}{1-\varepsilon^2}}-1\right]\frac{1}{\varepsilon}} \quad (22)$$

Where:

ε = The eccentricity

K_G = The load capacity coefficient

And for the segment bearing:

$$p_a = \frac{kMg+F_D+F_p}{\pi rL\left(\frac{A}{2(A-1)}\ln\frac{A}{2-A}-1\right)\left(1-\frac{1}{z^2}\right)\cos\frac{180^\circ}{z}} \quad (23)$$

The relative elongation for gas lubrication bearings rarely exceeds the limits determined by the technological accuracy λ = 0.5-2, relative eccentricity under load is usually ε = 0.6-0.9. The circumferential velocity on the shaft cannot be either low (due to reduction in load capacity with the decrease in Λ) or very high, since, its value has a rational limit, after which no increase in load capacity occur. Keeping the above mentioned in mind, we can select the values close to maxima for qualitative evaluation. For example, A = 1.8, λ = 1.5, E = 0.8, U = 150 m/sec.

If we apply these values to Eq. 22, we will obtain the following expression for the value of the bearing pressure of a full-radius bearing:

$$p_a = \frac{g}{4u^2\lambda\pi\sqrt{1+\frac{2}{3}\varepsilon^2}\left[\sqrt{\frac{1}{1-\varepsilon^2}}-1\right]\frac{1}{\varepsilon}} \quad (24)$$

$$M\omega^2 = 23*10^{-6}M\omega^2$$

where, ω is the rotational frequency. In the case of a four-segment bearing with the load directed between the segments, we will assume that A = 1.8 and L = λ*2r = 1.5 * 2r. If we apply these values to (Eq. 23), we will get:

$$p_a = \frac{g}{2\pi u^2\lambda\left(\frac{A}{2(A-1)}\ln\frac{A}{2-A}-1\right)\left(1-\frac{1}{4^2}\right)\cos 45^\circ} \quad (25)$$

$$M\omega^2 = 47{,}5*10^{-6}M\omega^2$$

Namely, the required pressure is almost doubled. Therefore, load capacity of a segment bearing is significantly lower than the full-radius one. In the case where the load falls onto the segment, the load capacity is further reduced. The coefficient in Eq. 25 will already be 64.3 for a four-segment GDSB when the resultant passes through one of the segments. Besides, as the number of segments increases, the overall load capacity decreases. Table 1 shows the results of calculating the coefficient in (Eq. 25) for the case when the resultant lies on a segment for a different number of segments.

Table 1: Value of the load capacity coefficient

Number of segments	1	2	3	4	5	6
Coefficient in the formula (4.19)×10^{-6}	23.0	42.0	53.0	64.3	82.0	103

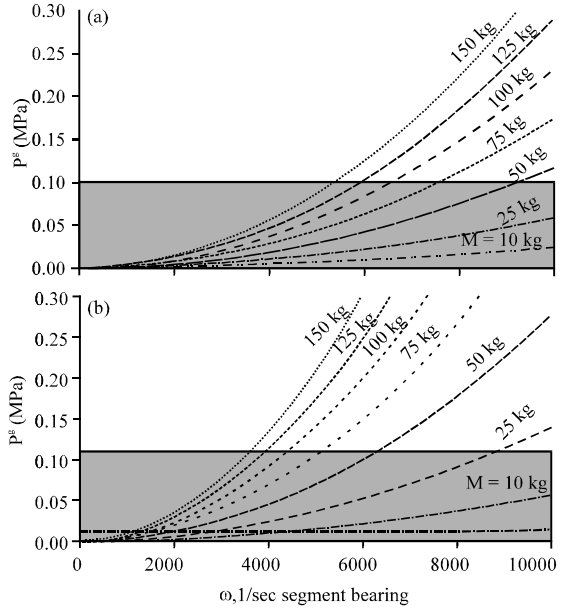

Fig. 2: Asymptotic evaluation of bearings load capacity and the dependence of the required bearing pressure on the shaft rotation frequency

If we increase the shaft velocity unlimitedly then the load capacity of the full-radius bearing will asymptotically tend to the limit and the load capacity of the segment bearing will be maximum.

Calculation results for required blowing pressure for different rotor masses depending on the rotor velocity are shown in Fig. 2.

It is clear that with the increase of mass and rotor velocity, the required bearing pressure continuously increases. The zone below the horizontal line of 0.1 MPa contains the rotors which can be equipped with bearings at atmospheric pressure, namely with GDBs. Rotors falling in the zone above this line must be equipped with bearings with additional air blowing into the lubricating gap, namely with GSDBs.

Asymptotic analysis of rotation frequency, at which the bearing starts working in a contactless mode: The shaft rotation velocity at which the shaft detaches from the

bearing is another criterion for choosing the type of gas bearing (GSB, GSDB or GDB). The above analysis showed that the smaller is this velocity, the smaller is the size of the output gap h_{out}. We recall that air bearings have a limiting regime at $\Lambda \to \infty$ such that a further increase in the rotational velocity does not lead to an increase in the load capacity. In this case, there are analytical expressions for the load capacity W for full-radius bearing:

$$W = 2rLp_a\pi\sqrt{1+\frac{2}{\varepsilon}\varepsilon^2}\left(\frac{1}{1-\varepsilon^2}-1\right)\frac{1}{\varepsilon} \quad (26)$$

For segment bearings with segment length d:

$$W = dLp_a\left(\frac{A}{2(A-1)}\ln\frac{A}{A-1}-1\right) \quad (27)$$

Based on Eq. 26-27, there is determined the size of the output gap for full-radius bearing:

$$hout = c(1-å) \quad (28)$$

and for segment bearing:

$$hout = h0(2-A)h_0 = \sqrt{\frac{6\mu ud}{\Lambda p_a}},\ u = \omega r \quad (29)$$

The h_{out} of a segment bearing depends on the Harisson criterion Λ, unlike the case of a full-radius bearing (Eq. 28 and 29). This should be explained. Let's assume that the segment bearing is designed in such a way that it has a certain value of the characteristic Λ under some load at the nominal rotation velocity. This characteristic will remain unchanged when the rotational velocity reduces because a constant pressure diagram in the lubricating layer will be required to compensate for the constant load. The diagram is in turn, determined by this characteristic's value. In other words, when the rotational velocity changes the value of h_{out} will change in such a way that the bearing's characteristic Λ will remain unchanged. Thus, Λ must be specified for a segment bearing. The experience in designing segment bearings known that Λ is usually assigned in the range of $\Lambda = 2.30$. Since, we analyze the detachment velocity, it is necessary to choose Λ as close as possible to the limit regime $\Lambda \to \infty$, therefore we set $\Lambda = 30$.

In the case of a radial full-radius bearing with reduced rotation velocity, the effective load will be compensated by the increase of eccentricity in such a way that the coefficient of load capacity will remain constant and therefore, the characteristic Λ will decrease in accordance with the expression:

$$\Lambda = \frac{K_\Gamma}{\pi}\frac{\left(2+\varepsilon^2\right)\sqrt{1-\varepsilon^2}}{\varepsilon} \quad (30)$$

According to Eq. 26-30, if h_{out} is equal to the minimum possible h_{min} then the bearing's detachment frequency can be determined by equation:

$$\omega_{OT} = \frac{c^2p_a}{6\pi\mu r^2}\frac{K_\Gamma\left(2+\left(1-\frac{h_{min}}{c}\right)^2\right)}{1-\frac{h_{min}}{c}}\sqrt{1-\left(1-\frac{h_{min}}{c}\right)^2} \quad (31)$$

(for a full-radius bearing) and for a segment bearing with the number of segments of z:

$$\omega_{OT} = \frac{(h_{min})^2 z\Lambda p_a}{6\mu r^2 2\pi(2-A)^2} \quad (32)$$

It is clear from Eq. 31 and 32 that by decreasing the maximum permissible value of $h_{ow} = h_{min}$, it is possible to substantially reduce the angular rotation velocity of the shaft at which it detaches from the bearing. Let us estimate the relationship between the rotational speed and the minimum gap for a typical case.

If we assume that A = 1.8, D = πr/2, U = 150 m/sec, Λ = 30, Pa = $0.1*10^6$ Pa, M = $1.8*10^{-5}$ Pa*s (for a four-segment bearing), we will obtain $h_{min} = 226\sqrt{1/\omega}\mu m$. Similarly, we assume that $\varepsilon = 0.8$ for a full-radius bearing (other parameters are the same). Thus, we will get $h_{min} = 180\sqrt{1/\omega}$

Thus, full-radius bearing requires a smaller output gap, therefore, it has more stringent requirements for accuracy of manufacturing. Consequently, segment bearing will be technologically simpler and cheaper.

Designing the radial nozzles of GSDB: If the segment rotates by some angle in a way that the width of the input and output gaps are different, there will be formed a pattern of pressure isolines (Fig. 3a). In Fig. 3a, the gas is supplied only through a nozzle with a rectilinear groove (Eq. 1) located at the exit section (right edge in the Fig. 3a).

Based on the calculations made for the segment with a single nozzle and on the asymptotic analysis performed in 1 and 2, we have chosen an average gap of

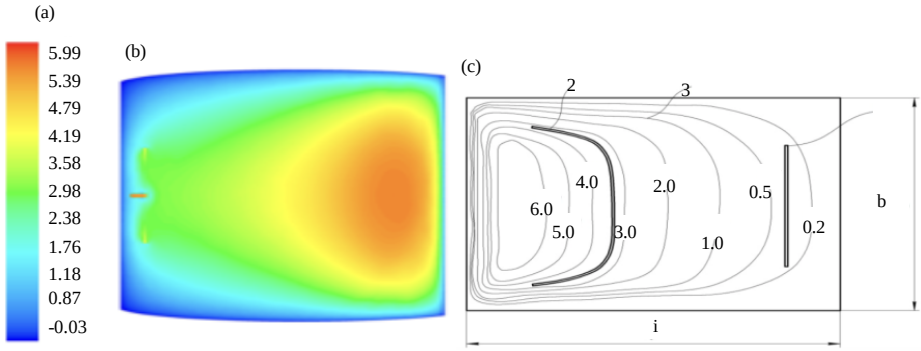

Fig. 3: a) Pressure distribution; b) along the bearing surface of a segment with the length l and width b and with a single slot nozzle 1. It was calculated with ANSYS CFX at shaft rotation velocity of 42.000 rpm at an average gap of 15 μm and a minimum gap of 7 μm and c) A scheme illustrates a sickle-shaped groove 2 along the isobar 3, pressure at which is equal to the pressure of the gas supply to the bearing

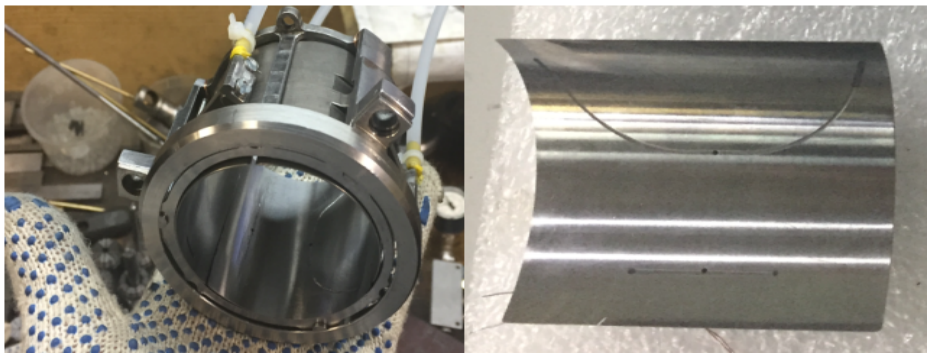

Fig. 4: a) The initial version of the radial GDSB and b) Its segment

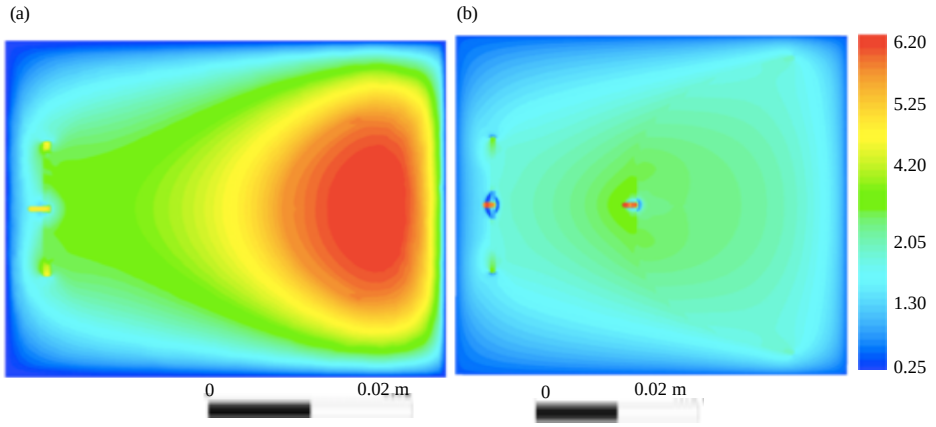

Fig. 5: a) Pressure distribution on designed and b)on test segments at the rotation velocity of 42.000 rpm and the average gap H_0 = 20 μm

H_0 = 15 μm for further calculations. Based on the graph above, we have found an output gap of h_{out} = 7.2 μm corresponding to a stable position. We have calculated the flow in the lubricating layer for a segment with one rectilinear canal in order to select the gaps. The line of sickle-shaped nozzle microgroove was plotted an isobar with a pressure of 6 bar was selected according to the pattern of pressure isolines.

At the end of the study, we have calculated the hybrid air bearing previously designed on the basis of data available from literature (Fig. 4). Figure 5a shows the

results of pressure distribution at the segment with the final nozzle geometry at the nominal regime. In this case, pressure profile is much more filled in comparison with the profile of the previously manufactured test bearing (Fig. 5b) and of the segment with one rectilinear nozzle (Fig. 3a). The load capacity of the newly designed segment is 25% greater than of the test one with the size of the average gap of 15-20 μm. This result is achieved due to the optimal geometry of the sickle-shaped nozzle.

Experimental verification of design results: We have performed a series of experiments was performed to test the developed methodology for GSDB design and mathematical modeling. Thus, we have determined the dependence of the load capacity of a radial GSDB on the shaft rotation velocity. The rotor of the apparatus rests on two gas GSDBs (radial-thrust one and the radial one) and is rotated by an air turbine. The rotation sensor controls its velocity, specified by the flow rate of the air supplied into the turbine. The studied radial GDSB is loaded via the rocker by the load device. During the experiment, the rotation velocity was set in the range of 10.000-42.000 rpm and the load on the shaft in the range of 500-700 N. The average gap controlled with an eddy current sensor was varied in the process.

CONCLUSION

Hybrid air bearings are an attractive area in the field of creating oil-free transmissions for rotary technology with heavy rotors or heavy load on the shaft. We have developed a methodology for designing self-aligning segments of such bearings as well as a technique applicable while calculating the moments of pressure forces acting on them. The gas must be fed into the gap at least through two nozzles in order to ensure the stability of segment's equilibrium position at which the moment on its rotation axis is zero. One of them was chosen straightforwardly based on the recommendations available from the literature while the geometry of the second one was determined by calculations. The study describes how the second nozzle's geometry and the flow in the lubricating layer were designed and mathematically modeled.

ACKNOWLEDGEMENT

This research was supported by Ministry of Education and Science of the Russian Federation (agreement No. 14.578.21.0203, ID RFMEFI57816X0203 for Applied Scientific Research).

REFERENCES

Beschastnykh, M.S. and T.E. Ilyina, 2015. Experience of designing bearings on gas lubrication. Refrig. Equipment, 1: 10-11.

Beschastnykh, V.N., 2011. Development of the calculation method and experimental determination of the characteristics of segmented radial gas bearings for heavy GTU rotors. Master Thesis, Gujarat Technological University, Ahmedabad, India.

Bulat, M.P. and P.V. Bulat, 2013. Basic classification of the gas-lubricated bearings. World Appl. Sci. J., 28: 1444-1448.

Constantinescu, V.N., 1963. [Gas Lubrication]. Editura Academiei Romane, Bucharest, Romania, (In Romanian).

Kotlyar, Y.M., 1967. Asymptotic solutions of the Reynolds equation. Fluid Dyn., 2: 104-106.

Nelson, D. and L. Hollingsworth, 1977. Radial bearing with self-aligning liners, equipped with liquid supports. Prob. Frict. Lubr. Ser. F., 1: 127-134.

Raimondi, A.A., 1961. A numerical solution for the gas lubricated full journal bearing of finite length. Asle Trans., 4: 131-155.

Reynolds, O., 1886. IV. On the theory of lubrication and its application to Mr. Beauchamp tower's experiments, including an experimental determination of the viscosity of olive oil. Philos. Trans. Royal Soc. London, 177: 157-234.

Sheinberg, S.A. and M.D. Shisheyev, 1979. Sliding Supports with Gas Lubrication. Mashinostroenie Publishers, Moscow, Russia,.

Stepanyants, L.G., 1967. Some methods of the Gas-dynamic theory of lubrication. Works Leningrad Polytech. Inst., 280: 27-43.

Sternlicht, B., 1961. Cylindrical sliding gas bearings of finite length. Appl. Mech., 28: 62-70.

Zablotsky, N.D., V.E. Karyakin and I.E. Spienkov, 1970. Spherical gas bearing with forced boost. Mech. Fluids, 3: 147-154.